Development 138, 4279-4290 (2011) doi:10.1242/dev.066480

Specific expression of a TRIM-containing factor in ectoderm cells affects the skeletal morphogenetic program of the sea urchin embryo

Vincenzo Cavalieri*, Rosa Guarcello and Giovanni Spinelli*

SUMMARY

In the indirect developing sea urchin embryo, the primary mesenchyme cells (PMCs) acquire most of the positional and temporal information from the overlying ectoderm for skeletal initiation and growth. In this study, we characterize the function of the novel gene *strim1*, which encodes a tripartite motif-containing (TRIM) protein, that adds to the list of genes constituting the epithelial-mesenchymal signaling network. We report that *strim1* is expressed in ectoderm regions adjacent to the bilateral clusters of PMCs and that its misexpression leads to severe skeletal abnormalities. Reciprocally, knock down of *strim1* function abrogates PMC positioning and blocks skeletogenesis. Blastomere transplantation experiments establish that the defects in PMC patterning, number and skeletal growth depend upon *strim1* misexpression in ectoderm cells. Furthermore, clonal expression of *strim1* into knocked down embryos locally restores skeletogenesis. We also provide evidence that the Otp and Pax2/5/8 regulators, as well as FGFA, but not VEGF, ligand act downstream to *strim1* in ectoderm cells, and that *strim1* triggers the expression of the PMC marker *sm30*, an ectoderm-signaling dependent gene. We conclude that the *strim1* function elicits specific gene expression both in ectoderm cells and PMCs to guide the skeletal biomineralization during morphogenesis.

KEY WORDS: TRIM, Sea urchin embryo, Ectoderm, Skeleton biomineralization, Morpholino oligonucleotides, Primary mesenchyme, Cell migration, Guidance, *otp*, *pax2/5/8*, *sm30*

INTRODUCTION

In the indirect developing urchins, the building of the embryonic endoskeleton is entrusted to the primary mesenchyme cells (PMCs), which are the sole descendants of the large micromere quartet of the 32-cell stage embryo (Wilt, 2002). At the blastula stage, the large micromere progeny undergoes an epithelial-mesenchymal transition and inhabits the blastocoel, forming the primary mesenchyme. Following ingression, PMCs extend numerous sensory filopodial protrusions that explore the inner face of the ectoderm (Gustafson and Wolpert, 1967; Malinda et al., 1995; Miller et al., 1995). After a brief random wandering phase, PMCs begin to migrate short distances along the extracellular matrix that lines the blastocoel cavity. Then, they gradually arrange themselves into a characteristic sub-equatorial ring pattern that surrounds the invaginating archenteron, with clusters close to two bilaterally symmetric thickenings in the ventrolateral ectoderm. By this time, PMCs are fused together to form a syncytium, and such a stereotypical organization imposes the skeleton morphology.

At the mid-gastrula stage, PMC clusters begin to crystallize two rhombohedral granules that elongate triradiate extensions (Okazaki, 1975a). As the skeletal rods grow, PMCs become spaced out along their length and, during later embryogenesis, the spicules increase in girth and branch in a stereotyped fashion, giving rise to the elaborated shape of the larval skeleton.

It is well established that large micromeres are autonomously programmed to give rise exclusively to skeletogenic cells (Angerer and Angerer, 2003; Ettensohn and Sweet, 2000; Okazaki, 1975b). Several genes encoding transcription factors and signal transduction molecules have been hierarchically structured into a model gene regulatory network that accounts for the specification program of the micromere-PMC lineage (Amore et al., 2003; Ettensohn et al., 2003; Oliveri et al., 2002; Oliveri et al., 2008; Röttinger et al., 2004). The initial activation of such a network relies on the interpretation of maternally derived anisotropies. In particular, in the newborn micromeres the nuclear β-catenin/TCF complex directly activates the zygotic expression of the transcriptional repressor Pmar1 (Oliveri et al., 2002), which sequentially prevents the expression of the repressor HesC, otherwise ubiquitously expressed (Revilla-i-Domingo et al., 2007). The resulting double-negative gate ensures the expression of the Notch-ligand Delta (Sweet et al., 2002) and a few regulatory genes, such as *alx1* (Ettensohn et al., 2003), *ets1* (Kurokawa et al., 1999) and *tbr* (Croce et al., 2001), exclusively in the PMC lineage. These genes encode transcriptional activators that, in turn, lead to expression of the suite of downstream skeletogenic genes. Recently, it has been elegantly demonstrated that transcription of *alx1* and *delta* genes occurs independently of the Pmar1/HesC control circuit (Sharma and Ettensohn, 2010), suggesting that the initial activation of the skeletogenic program is far more complex than was initially postulated.

Although the spicule formation process is determined entirely by the PMCs, the rate of spicule growth and the final shape of the skeleton are dictated by local ectoderm-derived cues (Armstrong et al., 1993; Ettensohn and Malinda, 1993; Guss and Ettensohn, 1997; Hardin and Armstrong, 1997). Old and recent evidence demonstrate that PMCs acquire most, if not all, of the positional and temporal information from the overlying ectoderm. Indeed, analysis of the filopodia extended from the PMCs indicate that they actively probe the inner face of the ectoderm and are responsive to directional cues (Malinda et al., 1995; Solursh and Lane, 1988).

Dipartimento di Scienze e Tecnologie Molecolari e Biomolecolari STEMBIO, Università di Palermo, Viale delle Scienze Edificio 16, 90128 Palermo, Italy.

*Authors for correspondence (vincenzo.cavalieri@unipa.it; giovanni.spinelli@unipa.it)

Accepted 21 July 2011

The molecular basis of the interplays between ectoderm and PMCs begins to be clarified. In a previous study, we demonstrated that Orthopedia (Otp), a homeodomain-class regulator expressed in a highly restricted manner in the ventrolateral ectoderm territory, is involved in epithelial-mesenchymal interaction and its expression specifically influences both the transcription of the PMC-specific *sm30* gene and skeletal patterning (Cavalieri et al., 2003; Di Bernardo et al., 1999). Combinatorial expression of further genes in discrete regions of the ectoderm is required to emanate short-range signals that direct the aggregation of subpopulations of PMCs into the bilateral clusters. Two of these signals have been recently identified as VEGF and FGF ligands (Duloquin et al., 2007; Röttinger et al., 2008). Both are expressed in two restricted areas of the ventrolateral ectoderm overlying the mesodermal clusters, whereas receptors are specifically expressed by the PMCs. The mentioned signal molecules trigger two disjoint and non-redundant pathways into the skeletogenic cells, and transduction of the information in both these pathways is specifically required for the expression of some late differentiation genes and for the expression of some late differentiation genes and for the skeletogenesis itself.

In this study, by gain-/loss-of-function and blastomere transplantation experiments we show that Strim1, a tripartite motif-containing (TRIM) protein, acts in restricted regions of the ventrolateral ectoderm as a novel regulator of the oriented migration and terminal differentiation of PMCs.

MATERIALS AND METHODS

Isolation of sea urchin strim1 cDNA and sequence alignment

A cDNA corresponding to the full-coding sequence of *strim1* was obtained by RT-PCR from a sample of total RNA extracted from *P. lividus* embryos at the gastrula stage. The oligonucleotide sequences were as follows: 5′-TCATATAGACTTTTCGTTATGG-3′ (forward) and 5′-TATCTAAA-TTGAATATATAAAGCCT-3′ (reverse).

Nucleotide sequence was verified and translated using the pDRAW32 software (http://www.acaclone.com). Putative protein domains were located via use of the Pfam (Finn et al., 2010) (http://pfam.sanger.ac.uk) and SMART (Letunic et al., 2009) (http://smart.embl-heidelberg.de) databases. The region of coiled-coil propensity was predicted by COILS version 2.2 (Lupas, 1996) (http://www.ch.embnet.org/software/COILS_form.html). Multiple sequence alignments were generated using ClustalW version 1.83 (Chenna et al., 2003) and the alignment output files were formatted using BioEdit version 7.0.9.

RNA extraction, Reverse-transcription, quantitative-PCR and whole-mount in situ hybridization

Total RNA from batches of unfertilized eggs and embryos grown at the desired stage was extracted, DNAse-treated and purified by phenol/chloroform extractions. Reverse-transcription and Q-PCR analysis were performed as described previously (Cavalieri et al., 2008; Cavalieri et al., 2009a). The oligonucleotide sequences, length, and amplicon size are described in Table S1 in the supplementary material.

Whole-mount in situ hybridization was performed adapting a procedure from Lepage (Lepage et al., 1992), whereas the double two-color whole-mount in situ hybridization procedure was as described (Thisse et al., 2004), with slight modifications.

Microinjection, embryo manipulation and imaging

Microinjection was conducted as described previously (Cavalieri et al., 2007; Cavalieri et al., 2009b). Either mRNAs or morpholino-oligomers were resuspended in 30% glycerol and, in selected experiments, Texas Red-conjugated dextran (Molecular Probes) was added at 5%. For overexpression experiments, capped mRNAs were synthesized from the linearized pCS2-constructs using the mMessage-mMachine kit (Ambion). Purified RNAs were resuspended at 0.5 mg/ml and 2 pl were then injected. Antisense morpholino-substituted oligonucleotides were obtained from Gene Tools (Philomath, OR). Nucleotide sequences were as follows: Mo-*strim1* 5′-TGGTGTTCTTTAATTCATCGGCCAT-3′ and Mo-*pax2/5/8* 5′-AAGTAGCCCGTCGGTGAAAATCCAT-3′. The control mInOtp-morpholino was previously described (Cavalieri et al., 2003). Approximately 2 pl of Mo-*strim1* and Mo-*pax2/5/8* solutions were injected into zygotes at final concentrations of 0.8-2.0 mM and 0.5-0.8 mM, respectively.

For both mRNA and morpholino microinjections, more than 150 injected embryos were observed and each experiment was repeated at least three times with different batches of eggs. Injected embryos at the desired stage were harvested, mounted on glass slides and examined under a Leica DM-4500B microscope. Images were captured with a Leica DC300F digital camera and processed using Adobe Photoshop CS4.

Transplantation of micromeres or halves recombination experiments were carried out as follows. Control or injected *P. lividus* embryos at the 16-cell stage were transferred into a modified Kiehart chamber in Ca^{2+}-free sea water and manipulated with fine glass needles under a Leica M165FC stereomicroscope equipped with micromanipulators (Narishige). After surgery, the embryos were returned to regular sea water and reared until the desired stage.

RESULTS

Cloning and sequence analysis of strim1 cDNA

The tripartite-motif (TRIM) domain is found in an increasing number of proteins with fundamental regulatory roles in cell differentiation and development (Meroni and Diez-Roux, 2005). We combined a sea urchin EST database scanning with standard RT-PCR to identify, in *Paracentrotus lividus*, a novel cDNA encoding a protein of 615 amino acid residues (Fig. 1A). Sequence analysis revealed characteristic domains classifying this protein as a member of the TRIM family, namely an N-terminal C3HC4-type RING-finger followed by two distinct B-box-type zinc-fingers and a coiled-coil domain (Fig. 1A). Both the RING and B-box domains contain all the invariant cysteine and histidine residues required for coordinating Zn^{2+} (Barlow et al., 1994; Freemont, 1993), whereas

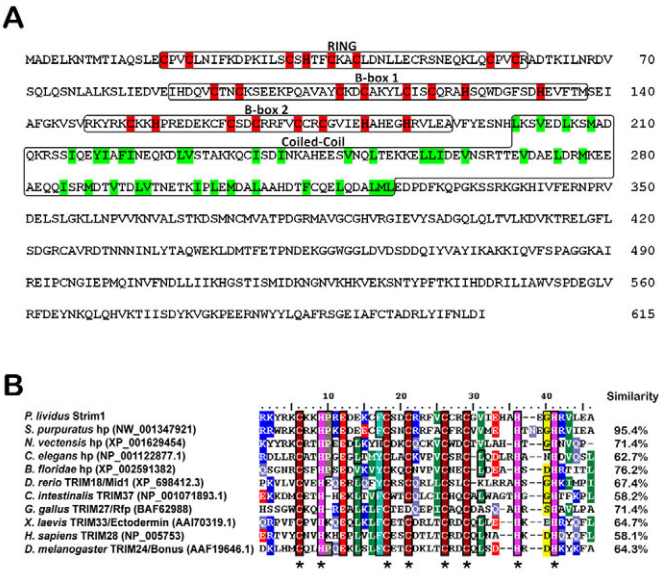

Fig. 1. Strim1 predicted amino acid sequence and B-box2 domain comparisons. (**A**) The zinc-binding residues of the N-terminal RING-finger and the two B-box domains are highlighted in red; hydrophobic residues are highlighted in green, within the coiled-coil domain. (**B**) Multiple comparison of the Strim1 B-box2 domain among species. Degrees of conservation (% similarity) are indicated on the right; residues involved in zinc coordination (100% conserved) are indicated by asterisks.

the coiled-coil domain contains several hydrophobic residues, as described for other member of the family (Lupas, 1996). No detectable conserved domains are located at the C-terminal region, so that the deduced protein groups with the subfamily C-V of TRIM proteins (Short and Cox, 2006).

The TRIM domain shows overall sequence similarity with a number of vertebrate TRIMs, and greater cross-species scores are observed when sequence comparisons are restricted to the RING or B-box domains (Fig. 1B). However, several attempts to conduct phylogenetic analysis using sets of TRIMs from various species gave ambiguous results (see Fig. S1 and Table S2 in the supplementary material). Therefore, in absence of a strong evidence for grouping this sequence with other known orthologs, we decided to name this Strim1 (sea urchin trim 1). Notably, the high degree of conservation seen between the *P. lividus* and the evolutionarily distant *S. purpuratus* species (Littlewood and Smith, 1995) (see Fig. S2 in the supplementary material) suggests that this protein has an important functional role in sea urchins.

Strim1 zygotic transcripts are confined exclusively into ectoderm cells

Strim1 is a zygotic gene that displays two major phases of expression. Its transcription begins at the 16-cell stage and, from the onset of primary mesenchyme ingression, transcripts abruptly increase in abundance and are maximally expressed at the gastrula stage. A lower level of transcription is detectable in the pluteus larva.

Whole-mount in situ hybridization showed that, at the 60-cell stage, *strim1* expression is restricted to the animal hemisphere, which gives rise to ectoderm territories (Fig. 2B). Following cleavage, the expression domain consisted of a wide region of the blastula epithelium (Fig. 2C), and largely overlaps with that of *nodal* (Duboc et al., 2004) on the oral side of the presumptive ectoderm (see Fig. S3 in the supplementary material). At the mesenchyme blastula (Fig. 2D) and gastrula (Fig. 2E,F) stages, *strim1* mRNA was mainly localized to two bilateral regions of the ventral ectoderm that foreshadow the sites of aggregation of the PMC clusters, where synthesis of the skeleton is initiated. Furthermore, in embryos at gastrula and prism stages, expression occurred also in a smaller region of the apical ectoderm (asterisks in Fig. 2F-H). At the early pluteus stage (Fig. 2I), *strim1* mRNA were found in ectoderm cells surrounding the tip of the growing arms.

Ectopic expression of strim1 disrupts PMC pattering and skeletal morphogenesis

To clarify the *strim1* function, we microinjected the synthetic mRNA into zygotes. As a control, eggs from the same batches were injected with equal amounts of a mutant frame-shifted *strim1* mRNA, and embryos developed normally (Fig. 3A,D). By contrast, almost all the embryos expressing the functional *strim1* exhibited highly reproducible strong perturbation of the skeletogenic program. Development of these embryos was apparently normal until the early gastrula stage. At this time, when control embryos displayed a regular ring with two bilateral clusters of PMCs (Fig. 3A), embryos translating exogenous *strim1* mRNA showed defective distribution of PMCs. In particular, although a subequatorial ring of mesenchyme cells was formed, additional clusters of PMCs were frequently visible (Fig. 3B). In other embryos (e.g. as shown in Fig. 3C), PMCs were quite homogeneously distributed around the archenteron, without distinguishable clusters.

A striking phenotype was even more apparent at the pluteus stage. Control embryos were normal larvae exhibiting the characteristic bilateral skeletal pattern (Fig. 3D). By contrast, although the basic spicule elements were formed, the vast majority of *strim1*-injected embryos presented an abnormal pattern of branching of the skeletal rods, whose growth followed an unpredictable pattern (Fig. 3E). Careful examination of some apparently normal embryos revealed aberrant duplications of either the anterolateral or postoral rods (Fig. 3F). A multi-branched effect is particularly evident in the specimen shown in Fig. 3G, in which an abnormal ramification of the ventral transverse rod provoked a comb-like arrangement of the skeleton in the oral side. A smaller fraction of the injected embryos (10%, n>1000) presented supernumerary triradiate spicules adjacently located to the oral side or close to the aboral vertex of the larva (Fig. 3H and I, respectively).

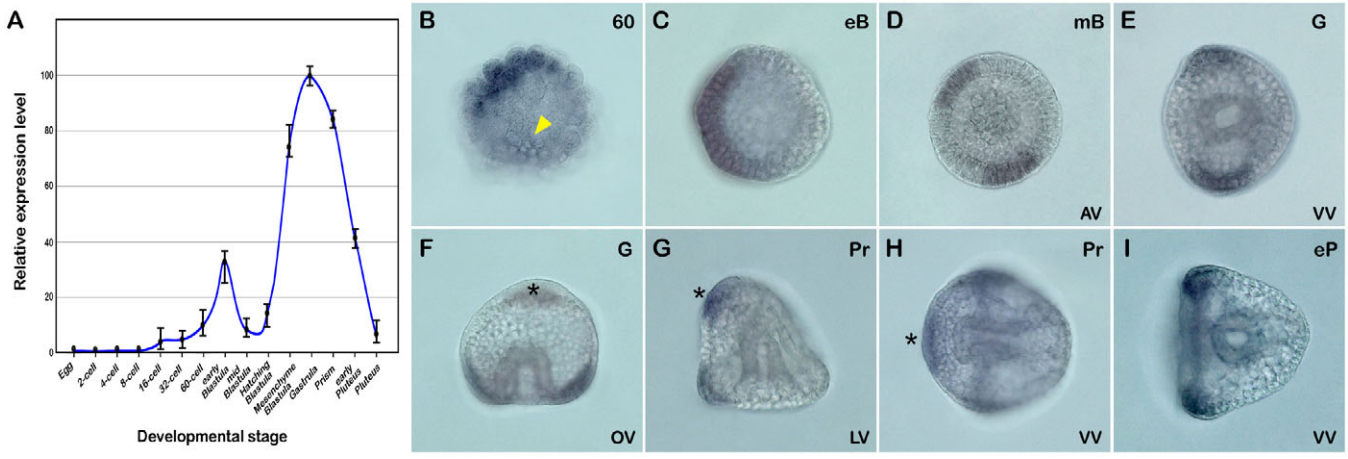

Fig. 2. *strim1* expression during embryogenesis. (**A**) Q-RT-PCR analysis. Values at the different stages are shown as a percentage of the maximum signal intensity. (**B-I**) Spatial distribution of the *strim1* transcripts revealed by whole-mount in situ hybridization. The arrowhead in B indicates the micromeres; asterisks in F-H indicate the animal region of *strim1* expression. 60, 60-cell stage; eB, early blastula; mB, mesenchyme blastula; G, gastrula; Pr, prism; eP, early pluteus; AV, animal view; VV, vegetal view with the oral side to the left; OV, view from the oral ectoderm; LV, lateral view with the animal pole at the top.

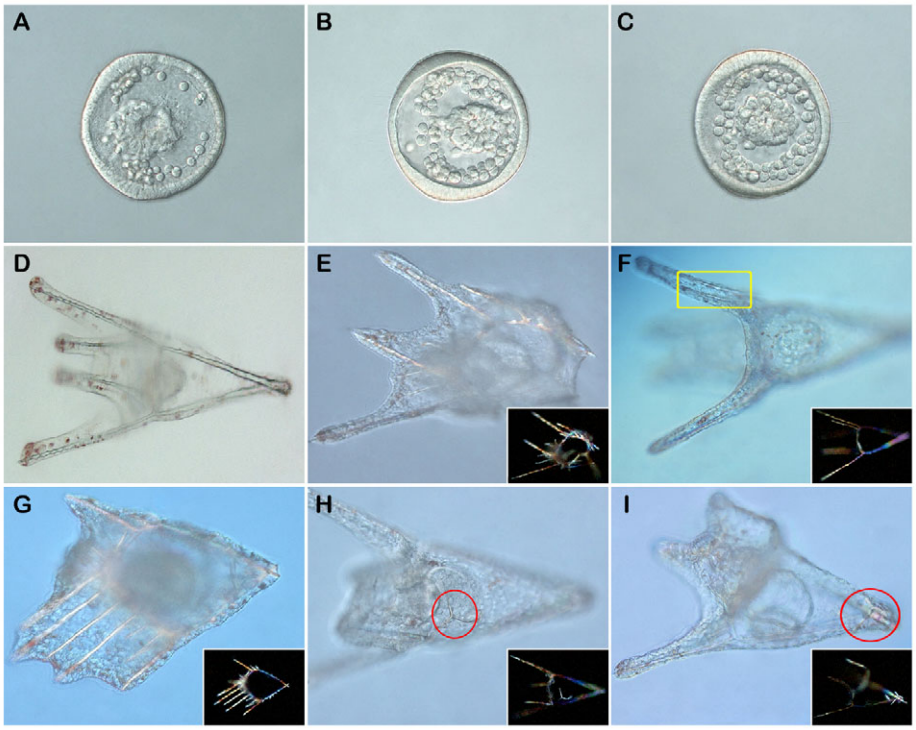

Fig. 3. Skeletogenic defects provoked by *strim1* overexpression. *strim1* mRNA was injected into zygotes and embryos were observed at the gastrula (A-C, ventral views) or pluteus stage (D-I); (A,D) control RNA-injected embryos. (**A-I**) DIC images; the lower right corners of E-I show the dark-field skeleton images (illuminated with plane-polarized light). Yellow square in F indicates an abnormal duplication of the postoral rod; red circles in H,I indicate supernumerary triradiate spicules.

We noted that in most of the injected embryos (70%, n>1000) the overall PMC number was remarkably higher than that of the control embryos (compare Fig. 3A with 3B,C). This observation was confirmed by whole-mount in situ hybridization with the PMC-specific marker *msp130*. As it can be seen in Fig. 4, late gastrulae overexpressing *strim1* contained an average of 65-70 PMCs, as opposed to the 30-34 marked cells normally present in control embryos at the same stage (Fig. 4A-C). A similar effect on PMC number was previously reported following overexpression of the *vegf* and *fgf* genes (Duloquin et al., 2007; Röttinger et al., 2008). We also noted that the expression level of the secondary mesenchyme cell marker genes *gcm* and *papss* (Ransick et al., 2002; Röttinger et al., 2006) did not significantly change in *strim1*-overexpressing embryos (Fig. 4J).

It did not escape to our attention that the spatial expression domain of *strim1* at gastrula stage is roughly coincident with that of marker genes that have been previously implicated in skeletogenesis, such as *otp*, *pax2/5/8*, *vegf* and *fgfA*. Because expression of *strim1* precedes the temporal activation of all these genes, we asessed their possible functional relationship. Indeed, *strim1* misexpression did correlate with a broadened ectopic transcription of *pax2/5/8* and *fgfA* in the ectoderm territory (Fig. 4D-I) of a fraction of *strim1*-injected embryos (70% and 30% respectively, n>100). By contrast, spatial distribution of the *vegf* transcripts was largely unaffected (n=77, data not shown). The mRNA abundance of these genes was examined by Q-PCR and, as expected, the *vegf* levels did not change significantly in *strim1* overexpressing gastrulae (Fig. 4J). Conversely, upregulation was detected for the other genes, with a conspicuously stronger effect on *otp* transcription. Because *otp* has been functionally related to the PMC-specific gene *sm30* (Cavalieri et al., 2003), we anticipated that *sm30* would be upregulated in *strim1*-injected embryos. Indeed, such a hypothesis was fully corroborated by Q-PCR analysis, with a ~12-fold increase in the *sm30* transcript level (Fig. 4J).

Transplantation of micromeres correlates skeletal abnormalities with strim1 misexpression in ectoderm cells

The effects of *strim1* overexpression suggest a defect in the interaction between the PMCs and the ectoderm. If this is the case, ectoderm cells expressing *strim1* should be able to affect the patterning of unperturbed PMCs. To demonstrate this, we generate chimeric embryos by swapping micromeres, at the 16-cell stage, from *strim1*-injected embryos with those explanted from GFP mRNA-injected embryos at the same stage (Fig. 5A). It follows that, in a developing chimera, PMCs appear green upon fluorescence observation, whereas *strim1*-expressing cells appear reddish, owing to the co-injection of Texas Red-conjugated dextran (TRCD). This double staining allowed us to verify that the transplant was successful and it also provided a means of examining the patterning of the micromere progeny into the blastocoel.

The reciprocal combination was also made and embryos observed at late gastrula stage. In almost all these embryos (n=9/10), the TRCD-labeled PMCs were located inside the blastocoel and were arrayed in a pattern consistent with that of undisturbed embryos (compare Fig. 5B with 5C). This result demonstrates that forced expression of *strim1* in the micromere lineage did not affect the behavior of the skeletogenic mesenchyme. By contrast, chimeric embryos containing control GFP-expressing PMCs and ectoderm derived from *strim1*-injected blastomeres exhibited a phenotype similar to that observed in *strim1*-injected non-chimeric embryos (compare Fig. 5D with 5E). Strikingly, although PMC clusters were still recognizable in these embryos, the overall number of skeletogenic cells was augmented with respect to the reciprocally recombinant embryos. Of 10 transplanted specimens, eight displayed this phenotype and showed irregular ramification of the skeleton at later stages of development (not shown). Taken together, our data support the hypothesis that misexpression of *strim1* in ectoderm cells impinges on the number and location of PMCs, as well as the subsequent skeletogenic process.

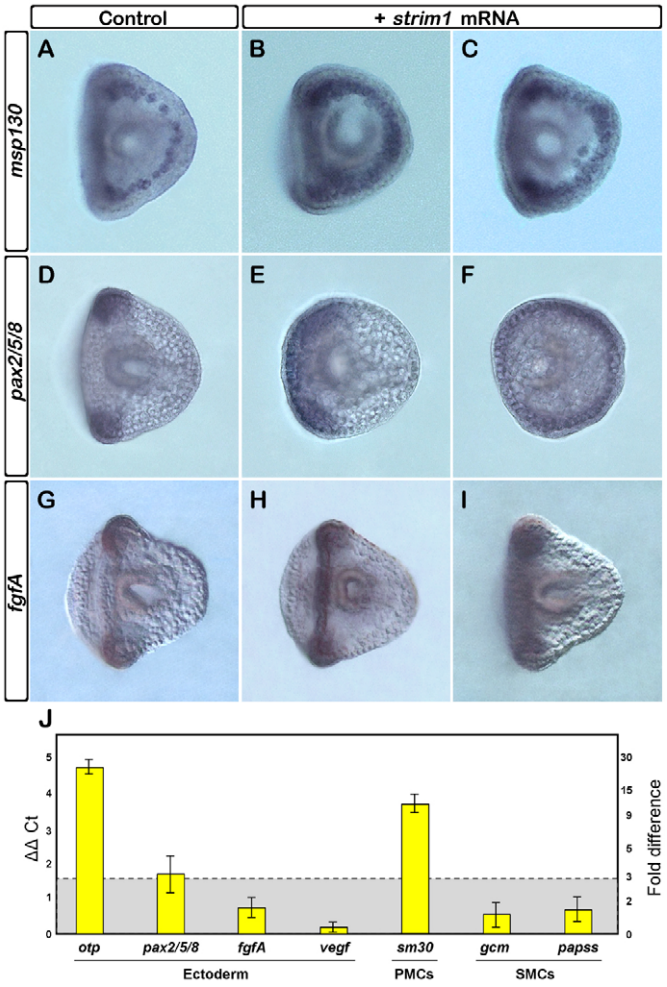

Fig. 4. Effects of *strim1* misexpression on marker genes transcription. (**A-I**) Embryos overexpressing *strim1* were fixed at the gastrula stage for whole-mount in situ hybridization with the indicated probes. (A,D,G) Control RNA-injected embryos. All embryos are oriented in a vegetal view. (**J**) Changes in gene expression levels assessed by Q-PCR in *strim1*-injected late gastrulae. Data are indicated as normalized ΔCt (ΔΔCt, left ordinate), and as the corresponding fold difference in transcript abundance (right ordinate), with respect to control injected embryos at the same stage of development. The gray region represents ΔΔCt values corresponding to non-significant variation (less than threefold difference). Error bars indicate s.e.m. for the Q-PCR replicates.

Inhibition of strim1 translation abrogates the PMC positioning and blocks skeletogenesis

To investigate in more detail the function of *strim1* during embryogenesis, we performed loss-of-function experiments by injecting a morpholino-substituted antisense oligonucleotide (Mo-*strim1*) (Summerton and Weller, 1997).

In a preliminary experiment, Mo-*strim1* efficacy in arresting translation in living embryos was evaluated using a construct in which the 5′UTR region of the *strim1* message, encompassing the ATG and Mo-*strim1* target sequence, was fused in-frame with the GFP coding sequence. As illustrated in Fig. 6A, the 5′*strim1*-GFP RNA injected embryos showed a diffuse fluorescence, indicating that the synthetic transcript was efficiently translated throughout the embryo. Conversely, the loss of GFP expression from each of the co-injected embryos (n>250) demonstrates that Mo-*strim1* specifically inhibited the production of the GFP protein in vivo (Fig. 6B). By contrast, bright fluorescent signal was detected from a similar number of embryos co-injected with Mo-*strim1* and an altered form of the *5′strim1*-GFP RNA, in which eight nucleotide changes in the Mo-*strim1* target sequence were introduced (Fig. 6C). As expected, injection of an unrelated morpholino together with the wild-type RNA did not detectably reduce the GFP-fluorescence (Fig. 6D).

To deprive embryos of the endogenous Strim1 protein, different batches of fertilized eggs were injected with Mo-*strim1* at concentrations ranging from 0.8 to 2.0 mM (preliminary experiments showed that Mo-*strim1* was either ineffective or non-specifically toxic at concentrations below 0.8 mM and above 2.0 mM, respectively). As expected, no deleterious effects were detected in almost all embryos injected with the same doses of the control morpholino (Fig. 6E-G). By contrast, Mo-*strim1*-injected embryos exhibited a range of reproducible phenotypes that were related to skeletal morphogenesis and were of increasing severity at higher concentrations (Fig. 6H-O). The most severely affected embryos displayed profound defects in the PMC patterning and endured a complete failure of the skeletogenic program (Fig. 6H-L). Careful microscopic observations indicated that, in these specimens, PMC ingression occurred on schedule with respect to control embryos (Fig. 6H). At later stages, however, despite the fact their number did not seem to be reduced, PMCs were irregularly dispersed into the blastocoel and did not synthesize calcareous elements. Although these embryos remained alive and swam regularly for several days, the full absence of the supporting skeletal framework resulted in embryos that appeared almost spherical, whereas control embryos displayed the distinctive angular shape of the pluteus larva. Although the gastrulation process occurred almost normally, the archenteron failed to connect the oral ectoderm so that the mouth almost never opened (90%, n>1000).

Some sibling embryos presented intermediate phenotypes with either only one little spicule forming on one side of the embryo (arrowhead in Fig. 6M), or two inadequate skeletal elements correctly allocated but disproportionate to one another (Fig. 6N). In other embryos, the body rod spicules extended parallel instead of converging toward the aboral apex, giving the embryos the characteristic shape of a chair (Fig. 6O).

All the repertoire of phenotypes described above was consistently observed in multiple trials, with one phenotype or the others prevailing in a given experiment depending on the batch of eggs and on the concentration of Mo-*strim1* injected. At lower doses (0.8-1.2 mM), the mild one was more frequently observed (40%, n>1000) together with several unaffected embryos, whereas at higher doses (1.5-2.0 mM) the extremely strong one prevailed (60%, n>1000; most of the remaining embryos showed the intermediate phenotypes).

PMC patterning and skeleton formation rely on strim1 expression in the animal hemisphere

Mo-*strim1* was injected into zygotes along with the TRCD-fluorescent tracer and then, at the 16-cell stage, animal and vegetal halves from these embryos were separated and recombined with their complementary halves derived from uninjected embryos (Fig. 7A). When Mo-*strim1* was contained only in vegetal halves, the resulting chimeras developed into normal plutei (n=9/10). In these embryos, descendants of vegetal cells normally formed the endomesoderm territories, which appeared red fluorescent (Fig.

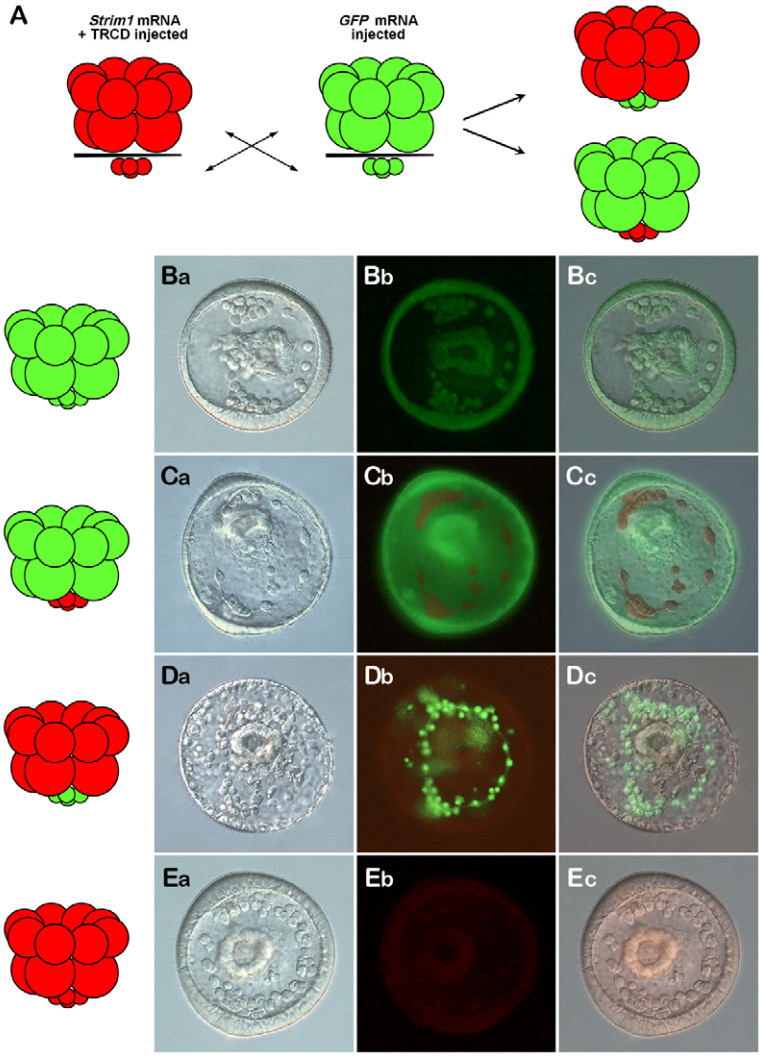

Fig. 5. Overexpression of *strim1* in chimeric embryos bearing unperturbed micromere-PMCs. (**A**) At the 16-cell stage, micromeres were removed and reciprocally transplanted from *strim1*/TRCD co-injected and control GFP-injected embryos. (**Ba-Ec**) Vegetal views of representative examples of chimeric (Ca-Dc) and non-chimeric (Ba-Bc, Da-Dc) injected embryos observed at the gastrula stage. The composition of the chimeras is shown in the diagrams the left. DIC, epifluorescence and merged images, respectively ordered from left to right, are shown for each embryo.

7B). In addition, micromeres bearing Mo-*strim1* produced PMCs that synthesized the typical endoskeleton (Fig. 7B). From this evidence, it can be argued that *strim1* is not required in the vegetal half for skeletogenesis. By contrast, the reciprocal chimeric embryos, in which *strim1* function is inhibited in the animal hemisphere, phenocopied the morphology of the non-chimeric Mo-*strim1*-injected embryos (Fig. 7C; n=10/12). These results demonstrate that inhibition of *strim1* in the animal hemisphere, where it is normally expressed, is sufficient to impede the establishment of the correct PMC arrangement and prevent skeletogenesis. In addition, these findings indicate that skeletogenic defects originate not in PMCs, but are due to a failure in the overlying ectoderm to provide adequate patterning information.

Genes correlated with skeletogenesis are differentially affected by strim1 knock down

The relationship between *strim1* and genes that have been involved in the ectoderm-to-mesenchyme communication was first assessed (Fig. 8). Strikingly, we found that *pax2/5/8* expression was almost totally abrogated in most of the Mo-*strim1* injected embryos (70%, n=40) at late gastrula stage (Fig. 8B). In the remaining embryos, *pax2/5/8* transcripts were barely detectable, but showed an anomalous unilateral localization in the ectoderm (Fig. 8C), with respect to the control embryos (Fig. 8A). The Q-PCR analysis (Fig. 8M), confirmed that *pax2/5/8* represents a downstream (probably indirect) target of *strim1* in ectoderm cells.

Because *pax2/5/8* transcription is positively regulated by *fgfA* signaling (Röttinger et al., 2008), we appraised whether, and to what extent, the injection of Mo-*strim1* reduced the *fgfA* expression. As shown in Fig. 8M, we observed a modest decrease in the abundance of *fgfA* transcripts in *strim1* morphants. Accordingly, *fgfA* downregulation occurred only in a small fraction (~20%, n>80) of the injected embryos. Notwithstanding this slight effect, *fgfA* transcription was selectively abolished or barely detectable in ectoderm cells but not in PMCs (Fig. 8D-F). A straightforward interpretation of these observations is that *strim1*, together with other factor(s), indirectly participates in the transcription of the *fgfA* gene, to achieve the maximum expression in ectoderm cells. By contrast, *vegf* transcription was largely unaffected (Fig. 8M; n=62) following *strim1* loss of function.

Remarkably, *otp* expression was almost totally inhibited in *strim1* knocked-down embryos (Fig. 8M), consistent with the idea that it primarily relies on *strim1* function.

To follow the behavior of the PMCs in Mo-*strim1* injected embryos, we examined the expression of the *msp130* and *sm30* markers. In control embryos at the late gastrula stage, *msp130*

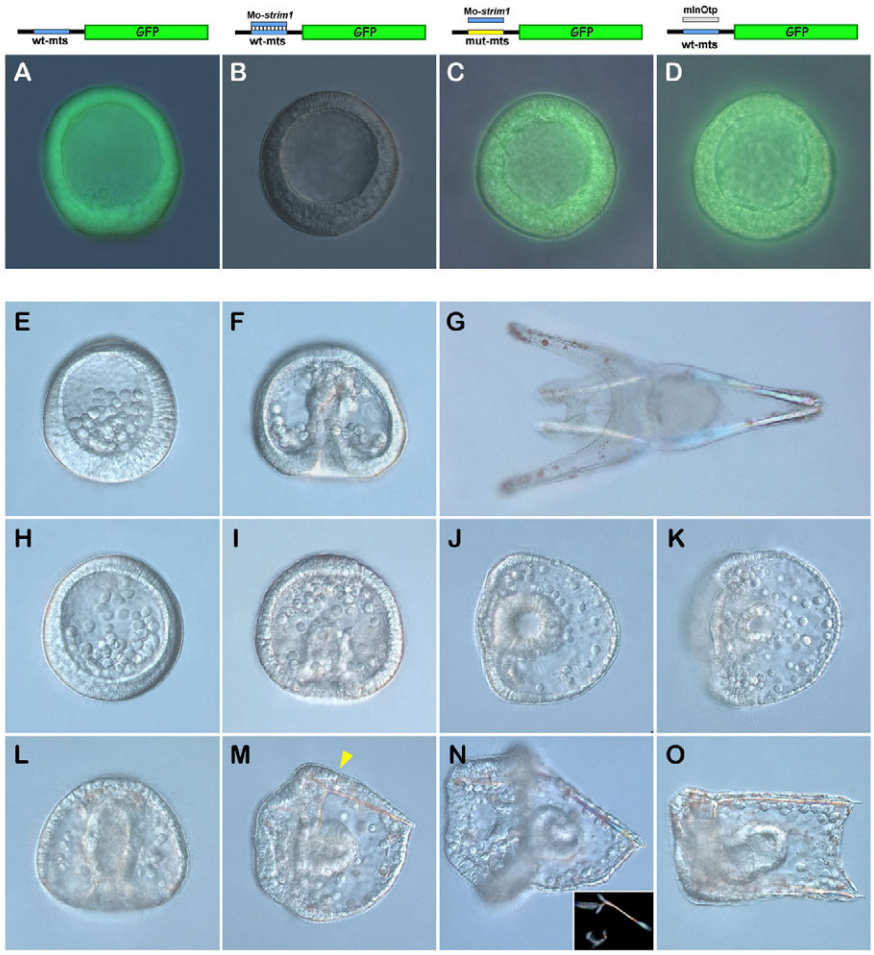

Fig. 6. Effects of *strim1* knock down on development. (**A-D**) Zygotes were co-injected with a synthetic GFP-encoding mRNA, that either contained a wild-type (A,B,D) Mo-*strim1* target-sequence (mts), or a mutated mts (C) in the 5′UTR, in combination with a 10,000-fold stochiometric excess of Mo-*strim1* or mInOtp. (**E-O**) DIC images of control (E-G) and morphant (H-O) embryos observed at 16 hours (E,H), 24 hours (F,I) and 60 hours (G,J-O) post-fertilization. Both the control and Mo-*strim1* were injected at 1.8 mM. A slight delay in gastrulation is observed in morphants at 24 hours of development (compare F with I), but this may not be a specific effect and in any case is only transient. The yellow arrowhead in M indicates the unique triradiate spicule. Inset in N shows the dark-field skeleton image.

messages were detected at almost equal level in all PMCs (Fig. 8G). At this stage, the transcription of *msp130* is known to be insensitive to extrinsic cues, probably being part of the autonomous program of the PMCs (Carson et al., 1985; Guss and Ettensohn, 1997). Accordingly, we found that the transcript level of *msp130* was not significantly altered by the loss of *strim1* function (Fig. 8H-I; n=45/50). We confirmed that in the morphants the complement of PMCs was fairly congruent with that of control embryos at the same stage but, in most of embryos (70%), the distribution of PMCs into the blastocoel was disorganized (Fig. 8H).

In normal gastrulae, *sm30* is expressed by all the PMCs, with a bias toward the ventrolateral clusters (Fig. 8J). Several lines of evidence demonstrate that *sm30* expression is tightly coupled to the deposition of skeletal elements and is strictly dependent upon signals emanating from the ectoderm (Cavalieri et al., 2003; Duloquin et al., 2007; Röttinger et al., 2008). In close agreement, we found that in *strim1* morphants the expression of the *sm30* gene was drastically downregulated, as indicated by whole-mount in situ hybridization (Fig. 8K; n=28/30) and confirmed by Q-PCR (Fig. 8M). Occasionally, *sm30* transcripts were barely detectable in few PMCs (arrowhead in Fig. 8L). Q-PCR measurements also revealed that the transcript abundance of *gcm* and *papss* genes was largely unaffected in Mo-*strim1*-injected embryos (Fig. 8M).

Altogether, these data strongly indicate that *strim1* is necessary for the proper positioning of the PMCs into the blastocoel. Furthermore, *strim1* is probably not required for PMC specification, but is most likely to be essential for turning on the expression of terminal differentiation genes, such as *sm30*, that are associated with the inception of the skeletal morphogenesis.

A localized source of strim1 restores skeletal biomineralization in strim1 morphant embryos

We performed a rescue assay in which a localized source of *strim1* was superimposed on morphant embryos. To avoid inhibition of the translation of the exogenous *strim1* mRNA by the morpholino, we conceived a synthetic *strim1* mRNA (m8-*strim1*), in which eight mutations in the sequence recognized by Mo-*strim1* were introduced. In the rescue experiment, Mo-*strim1* was first microinjected into zygotes along with TRCD, to discriminate among injected embryos and those that escaped microinjection (not-fluorescent). At the eight-cell stage, the m8-*strim1* RNA was successively injected into a single randomly chosen blastomere of TRCD-stained embryos (Fig. 9A). To follow the fate of the re-injected cells, the m8-*strim1* mRNA was delivered together with the GFP mRNA. As *strim1* is normally expressed in animal-derived cells, developing embryos displaying GFP fluorescence in the ectoderm were selected for microscopic observations. As expected, a sister batch of GFP-injected embryos, observed at the prism stage, developed normally (not shown). Conversely, a significant fraction of the double-injected embryos (53%, n>250) displayed a round-shaped morphology (Fig. 9B). In each of these embryos, PMCs entered the blastocoel and arranged themselves into a large aggregate where a single triradiate spicule was formed

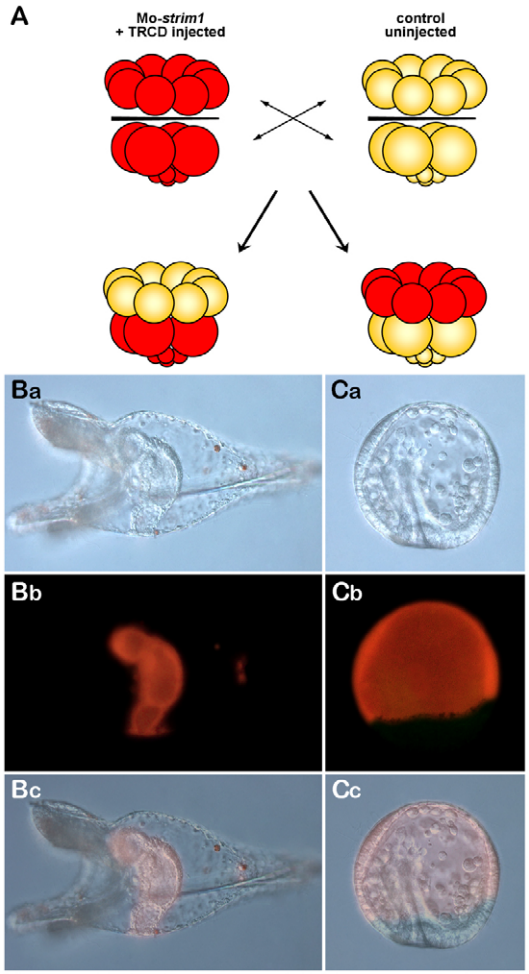

Fig. 7. Reciprocal recombination of animal halves between *strim1* morphants and unperturbed embryos. (**A**) At the 16-cell stage, animal and vegetal halves of co-injected Mo-*strim1*/TRCD and control uninjected embryos were isolated and recombined. (**Ba**-**Cc**) Side views of the resulting chimeras examined at 48 hours post-fertilization. DIC, epifluorescence and merged images, respectively ordered from top to bottom, are shown for each embryo.

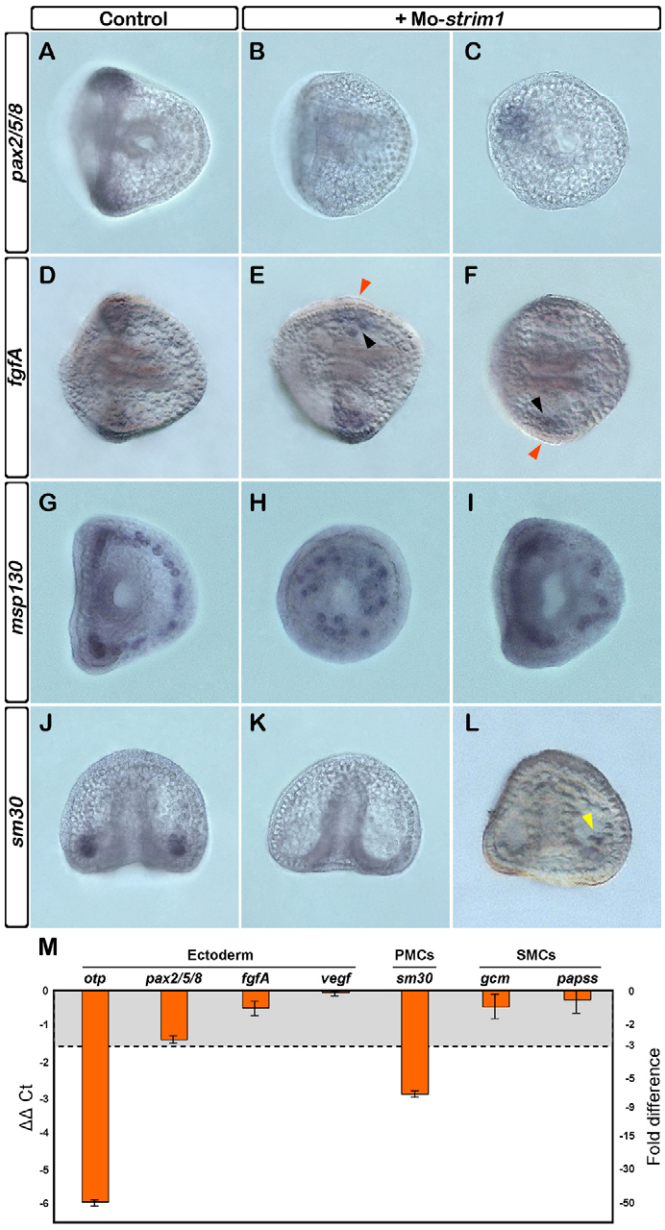

Fig. 8. Expression of marker genes in embryos bearing Mo-*strim1*. (**A-L**) Mo-*strim1* injected embryos were fixed at gastrula stage and analyzed by whole-mount in situ hybridization with the indicated probes. (A,D,G,J) Control embryos. (A-I) Vegetal views; (J-L) lateral views. Black and red arrowheads in E and F, respectively, indicate specific *fgfA* staining in PMCs and the absence of *fgfA* transcripts in the overlying ectoderm. Yellow arrowhead in L indicates specific *sm30* staining in few PMCs. (**M**) Changes in gene expression levels assessed by Q-PCR in Mo-*strim1*-injected late gastrulae. Data are mean±s.e.m.

(Fig. 9B-C). Inspection of these embryos under fluorescence illumination clearly revealed that the location of the PMC cluster, together with the embedded spicule, was in strict correspondence of the patch of GFP-staining and therefore of the ectoderm area expressing *strim1* (Fig. 9Bb-C). Importantly, this result confirms that the clone of *strim1*-expressing cells was capable of attracting the PMCs and influencing their behavior, which induced the elaboration of the skeletal element.

To obtain further insights on the relationship between *strim1* and skeletogenesis, we assessed (by whole-mount in situ hybridization) the expression of the *sm30* and *pax2/5/8* genes in the clonally rescued embryos. In each experiment, either the *sm30* or *pax2/5/8* probes were hybridized along with a fluorescein-labeled probe targeting the GFP transcript, to identify univocally the cells expressing exogenous *strim1*. As expected, *sm30* was found to be expressed exactly in the PMC aggregates adjacent to the ectoderm patches expressing GFP/*strim1* (Fig. 9D-E). Of importance, the rescued embryos also showed an almost perfect correspondence in the spatial expression domain of GFP/*strim1* and *pax2/5/8* (Fig. 9F-G). Taken together, these findings strongly point a role of *strim1* in directing skeletogenesis by affecting the expression of *sm30* and *pax2/5/8* genes.

To obtain more information on the role of *pax2/5/8* during morphogenesis, we blocked its function by injecting a morpholino oligomer (Mo-*pax2/5/8*), directed against the translation initiation codon. Remarkably, most of the Mo-*pax2/5/8*-injected embryos (70%, n>300) exhibited a phenotype similar to that observed

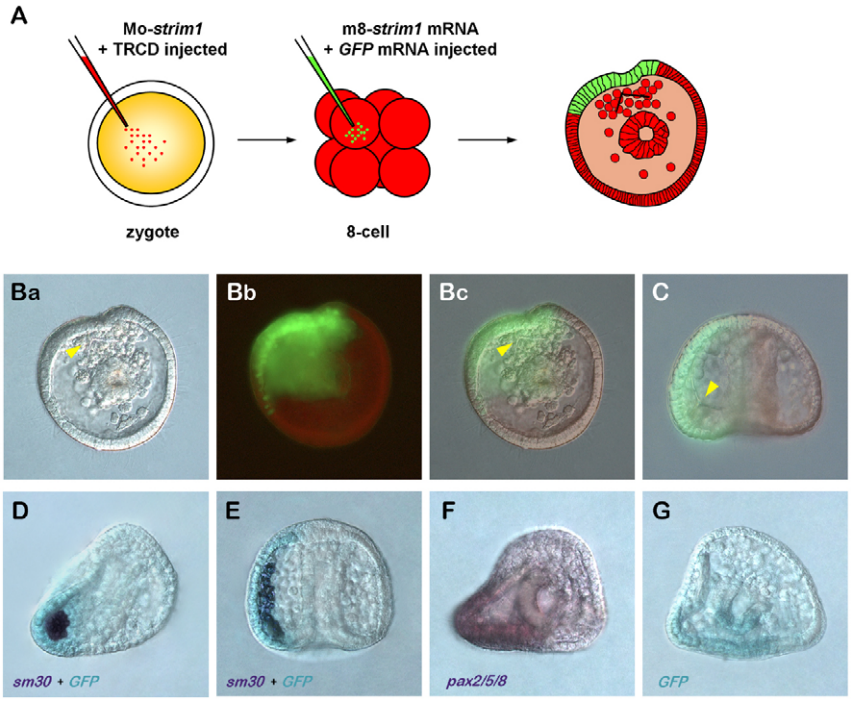

Fig. 9. Rescue of spicule biomineralization by *strim1* clonal-expression into *strim1* morphants. (**A**) At the eight-cell stage, one blastomere of Mo-*strim1*/TRCD embryos was co-injected with GFP and m8-*strim1* mRNAs. The resulting embryos were processed after 30 hours of development. (**Ba-C**) Representative examples of rescued embryos examined by DIC and fluorescence light. Yellow arrowheads indicate a triradiate spicule. (**D-G**) Embryos of sister batches analyzed by double two-color whole-mount in situ hybridization with the indicated probes.

following injection of the higher doses of Mo-*strim1* (Fig. 10D,E). Unexpectedly, after 48 hours of development PMCs of these embryos displayed a partial recovery in their biomineralizing activity. Indeed, two triradiate rudiments were formed apparently in correct positions (Fig. 10F), but they did not elongate as much as those of the control embryos at the same stage.

Subsequently, we overexpressed *pax2/5/8* following injection of the functional mRNA into zygotes. The resulting embryos developed almost normally up to the gastrula stage and contained the regular cohort of PMCs (Fig. 10G). At later stages, however, we found that almost all the injected embryos (>95%, n>250) showed complex branching of the skeletal rods (Fig. 10H,I), indicating that *pax2/5/8* interferes with the normal ramification of the growing skeleton. Furthermore, co-injection into zygotes of Mo-*pax2/5/8* and a *pax2/5/8* mRNA mutated in the morpholino target sequence led to a full recovery of spicule formation but provoked complex irregular branching (not shown).

Altogether, these results predict that supplying exogenous *pax2/5/8* might rescue some of the skeletal abnormalities caused by blocking of *strim1* translation. Indeed, the results showed in Fig. 10J-L fulfilled this assumption, as co-injection of the functional *pax2/5/8* mRNA along with Mo-*strim1* rescues an almost normal overall shape in more than 80% of embryos (n>400) observed at pluteus stage (as a yardstick, only less than 40% of the *strim1* morphants was able to synthesize skeletal elements, but they were single or disproportionate pairs of spicules). However, in most of the rescued embryos, the ectopic expression of *pax2/5/8* renewed the ability to form a basic skeleton but produced irregular branching (Fig. 10K,L). Remarkably, full rescue of the skeleton synthesis was also observed following co-injection of a functional *otp* mRNA along with Mo-*strim1* (see Fig. S4 in the supplementary material), although the ectopic expression of *otp* provoked a radial distribution of supernumerary skeletal rods around the archenteron, as previously described (Di Bernardo et al., 1999).

We conclude that, although the exact molecular function of Strim1 is actually not known, *strim1* expression is able to affect positively both *pax2/5/8* and *otp* gene expression in ectoderm cells to guide PMC positioning and skeletal biomineralization during morphogenesis.

DISCUSSION

Strim1, a TRIM-containing factor in the sea urchin embryo

The TRIM gene super-family encodes proteins involved in a broad range of cellular and developmental processes. For example, it has been recently shown that TRIM11 controls the endogenous level of Pax6 in the developing cortex of mice, so that block of TRIM11 function ultimately impairs Pax6-dependent neurogenesis (Tuoc and Stoykova, 2008). In *Xenopus laevis*, TRIM33/Ectodermin is essential for the specification of the ectoderm germ layer and acts by restricting the mesoderm-inducing activity of TGFβ signals to the mesoderm and favoring neural induction (Dupont et al., 2005). TRIM36/Haprin mRNA is instead enriched in the vegetal cortex of *Xenopus* oocytes and required for cortical rotation, dorsal axis determination and somite arrangement (Cuykendall and Houston, 2009; Yoshigai et al., 2009). In chick and rat, both TRIM32 and TRIM54/Murf1 expression is induced during myogenic differentiation and impairing of their function has been linked with forms of muscular dystrophy (Bodine et al., 2001; Kudryashova et al., 2005).

In this study we have characterized *strim1*, the first echinoderm member of the TRIM family. We provide multiple lines of evidence supporting a key role of *strim1* in the embryonic skeletal morphogenesis, although the molecular mechanism underlying the action of *strim1* in such a developmental process remains to be clarified. As described, Strim1 exhibits a characteristic multi-domain structure that could suggest a conserved function. In other TRIMs, the RING finger, either alone or in combination with the B-box domains, has been found to play a crucial role in mediating

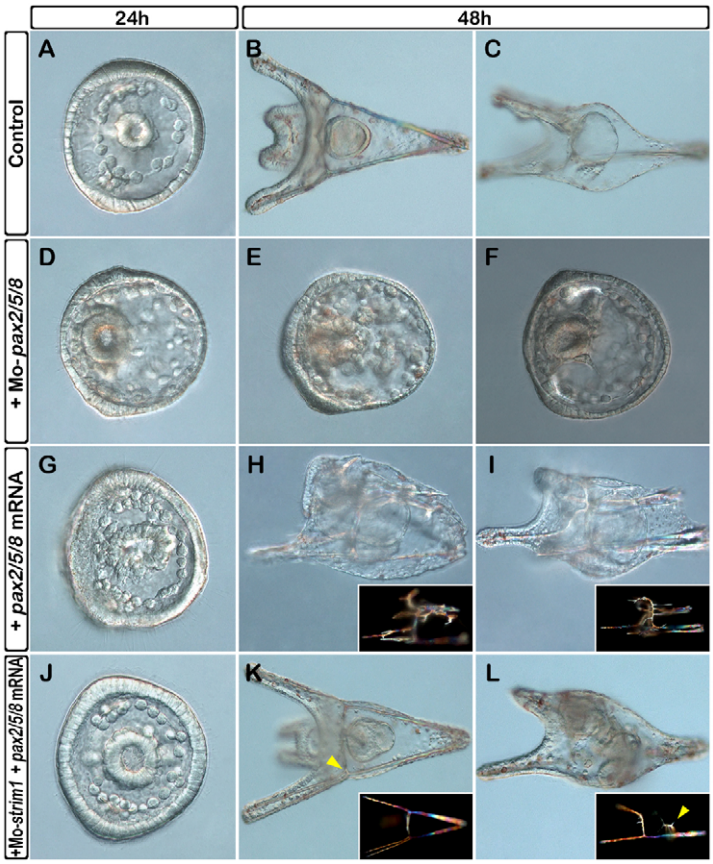

Fig. 10. Functional correlation between *strim1* and *pax2/5/8*. (**A-I**) Control (A-C), Mo-*pax2/5/8* (D-F) and *pax2/5/8* mRNA (J-L) injected embryos observed at gastrula (A,D,G) and pluteus (B,C,E,F,H,I) stages. (**J-L**) Representative examples of embryos rescued by co-injection with Mo-*strim1* and *pax2/5/8* mRNA. (A-L) DIC images; the lower right corners of H,I and K,L show the dark-field skeleton images. Arrowheads in K and L, respectively, indicate an abnormal duplication of the postoral rod and an extra spicule.

the transfer of ubiquitin to heterologous substrates, as well as to the TRIMs themselves (Gack et al., 2007; Joazeiro and Weissman, 2000). This domain could represent a signature of E3-ubiquitin-ligase activity. Similarly to Strim1, other TRIMs mediate cellular processes by regulating gene transcription, but the RING domain itself is not thought to be involved in specific DNA binding (Borden and Freemont, 1996). Rather, the protein-binding domains of the tripartite module are thought to specify the effector function, either by recruiting an additional co-factor or by participating in multimeric complexes (Diaz-Griffero et al., 2006). For example, the B-box domain associates with many other motifs and, likewise, the coiled-coil domain is known to be essential for both homo- and hetero-multimerization of many TRIMs (Perez-Caballero et al., 2005).

Strim1 and regulation of the skeletal morphogenesis

Results described in this paper correlate well with old and new evidence demonstrating that the skeletal morphogenesis results from the interplay between the intrinsic properties of the PMCs and the influence from the overlying ectoderm. The embryo probably does not regulate skeletal patterning simply by controlling sites of *strim1* expression, as *strim1* transcripts accumulate in a wide ectoderm region of the early embryo. However, at the onset of skeletal morphogenesis *strim1* is localized in the right place, being expressed in ectoderm regions adjacent to the bilateral clusters of PMCs. In addition, misexpression of *strim1* leads to severe skeletal abnormalities. Micromere transplantation experiments established that the defects in PMC patterning and spiculogenesis must be ascribed to the ectoderm. Indeed, although the injected *strim1* mRNA is likely translated in PMCs through gastrulation, its expression is irrelevant to the PMC behavior. These mesodermal cells are capable of migrating on schedule and eventually form spicules, the shape of which is congruent with that of unperturbed embryos.

Intriguingly, our results reveal a potential *strim1*-dependent control of the PMC number. Indeed, chimeric embryos overexpressing *strim1* in the whole ectoderm, but not in the PMCs, produced an approximately double complement of skeletogenic cells. Therefore, *strim1* expression might induce either an additional round of PMC proliferation or the alternative change in fate of other endomesoderm. We are fairly confident that this effect is not implicated with the skeletal abnormalities generated in these embryos. In fact, it has been shown that embryos transplanted with up to three times the normal number of PMCs form a skeleton of normal size and scale (Armstrong et al., 1993; Ettensohn, 1990).

We also showed that impairing *strim1* translation interferes with the correct migration pattern and terminal differentiation of the PMCs and, as a consequence, lead to absence of skeleton. The specificity of action of *strim1* is shown by mRNA injection effects in perturbed embryos. Indeed, clonally ectoderm-localized expression of *strim1* is necessary and sufficient to reactivate the skeletogenic program, as early attested by the exclusive expression of the *sm30* gene in the adjoining PMCs. Of relevance, these cells also resume the outstanding ability to migrate and point towards the ectodermal clone of *strim1* expression, indicating an involvement of *strim1* in regulating PMC guidance. This finding is in full agreement with that outlined in several previous studies indicating that the guidance of PMCs, as well as the subsequent spicule deposition, are heavily influenced by signals from the

ectoderm (Armstrong et al., 1993; Ettensohn and Malinda, 1993; Gustafson and Wolpert, 1967; Hardin et al., 1992). In this regard, cell migration to the ventral midline provides one of the best examples of TRIM-dependent regulation of guidance during embryogenesis. In *C. elegans*, TRIM18/MADD-2 functions to direct muscle and axon extensions to the ventral midline motor axons to form the postsynaptic membrane of the neuromuscular junction (Alexander et al., 2010).

Strim1 and the epithelial-mesenchymal gene regulatory network

We propose that *strim1* is part of the complex system of regulative interactions that bridge the ectoderm network, which has recently begun to be deciphered (Chen et al., 2011; Saudemont et al., 2010; Su, 2009), to the micromere-PMC network. Results presented here are in agreement with this hypothesis. First, throughout our experimental assays, *pax2/5/8* transcription and spicule deposition were always correlated with *strim1* expression, being both permitted in presence of a source of *strim1*, and rather impeded in embryos in which *strim1* function was impaired. Recently, the Lepage group has shown that functional FGF-A signaling pathway is required for *pax2/5/8* expression in the ectoderm regions surrounding the tip of the growing arm rods, and postulated an involvement of the Pax2/5/8 regulator in skeletal rod elongation (Röttinger et al., 2008). Our results are in agreement with this assumption and also suggest that *strim1* indirectly participates in the transcription of *fgfA* (see below).

Another effect of *strim1* is on the *sm30* PMC-specific gene expression. In this case, the influence is obviously indirect, as these genes are expressed in two distinct cell types. Similarly to that reported for *pax2/5/8*, we showed that *sm30* expression specifically occurred in a *strim1*-dependent manner. It is well documented that *sm30* uniquely responds to the local control of the ectodermal epithelium, and high levels of *sm30* transcripts are directly correlated to the deposition of spicule rudiments (Ettensohn et al., 1997; Guss and Ettensohn, 1997). We have shown elsewhere that *sm30* transcription relies on the expression of the Otp regulator in few bilaterally symmetric ectoderm cells (Cavalieri et al., 2003). The results presented in this paper suggest that *otp* transcription strictly depends upon *strim1* expression, being strongly upregulated or nullified after *strim1* gain- and loss-of-function, respectively. These findings lead us to presume that the effect of *strim1* perturbations on *sm30* gene expression is probably primarily exerted through *otp* dysregulation in the ectoderm. However, both Strim1 and Otp are likely to act within the ectoderm cells in which they are expressed. It follows that any effect on the underlying PMCs must therefore be indirect through secreted factors. It has been recently shown that the VEGF and FGF-A ligands, emitted by ventrolateral ectoderm cells, act as permissive short-range signals, being selectively perceived and transduced from PMCs to promote *sm30* expression (Duloquin et al., 2007; Röttinger et al., 2008). As judged by the whole-mount in situ hybridization data, the spatial expression pattern of *strim1* probably overlaps that of *vegf* and *fgfA*, but *strim1* transcription initiates earlier. The mentioned genes are functionally non-redundant, but the expression of each of them is equally required for the correct skeletal morphogenesis. We show that *strim1* function is sufficient, but not strictly necessary, to evoke *fgfA* gene expression in ectoderm cells. Rather, Strim1 participates marginally, together with other factor(s), in the expression of the *fgfA* gene. The functional characterization of the *cis*-regulatory apparatus of the *fgfA* gene should help to fulfill this hypothesis. Finally, our findings also rule out an involvement of *strim1* in *vegf* gene transcription. Nevertheless, we cannot fully exclude that the Strim1 factor could modulate the trafficking or protein stability of the VEGF and/or FGF-A ligands, as well as other secreted signaling molecules. Hopefully, identification of *strim1* regulators and partners will help to unravel the molecular mechanisms, and their hierarchical interconnections, that regulate the skeletal morphogenesis in the sea urchin embryo.

Acknowledgements
We thank Thierry Lepage for the *nodal* and *msp130* cDNA probes, and anonymous reviewers for their valuable suggestions and comments.

Funding
This work was funded by grants from the University of Palermo (ex60%).

Competing interests statement
The authors declare no competing financial interests.

Supplementary material
Supplementary material for this article is available at
http://dev.biologists.org/lookup/suppl/doi:10.1242/dev.066480/-/DC1

References

Alexander, M., Selman, G., Seetharaman, A., Chan, K. K., D'Souza, S. A., Byrne, A. B. and Roy, P. J. (2010). MADD-2, a homolog of the Opitz syndrome protein MID1, regulates guidance to the midline through UNC-40 in *Caenorhabditis elegans*. *Dev. Cell* **18**, 961-972.
Amore, G., Yavrouian, R. G., Peterson, K. J., Ransick, A., McClay, D. R. and Davidson, E. H. (2003). Spdeadringer, a sea urchin embryo gene required separately in skeletogenic and oral ectoderm gene regulatory networks. *Dev. Biol.* **261**, 55-81.
Angerer, L. M. and Angerer, R. C. (2003). Patterning the sea urchin embryo: gene regulatory networks, signaling pathways, and cellular interactions. *Curr. Top. Dev. Biol.* **53**, 159-198.
Armstrong, N., Hardin, J. and McClay, D. R. (1993). Cell-cell interactions regulate skeleton formation in the sea urchin embryo. *Development* **119**, 833-840.
Barlow, P. N., Luisi, B., Milner, A., Elliott, M. and Everett, R. (1994). Structure of the C3HC4 domain by 1H-nuclear magnetic resonance spectroscopy. A new structural class of zinc-finger. *J. Mol. Biol.* **237**, 201-211.
Bodine, S. C., Latres, E., Baumhueter, S., Lai, V. K., Nunez, L., Clarke, B. A., Poueymirou, W. T., Panaro, F. J., Na, E., Dharmarajan, K. et al. (2001). Identification of ubiquitin ligases required for skeletal muscle atrophy. *Science* **294**, 1704-1708.
Borden, K. L. B. and Freemont, P. S. (1996). The RING finger domain: a recent example of a sequence-structure family. *Curr. Opin. Struct. Biol.* **6**, 395-401.
Carson, D. D., Farach, M. C., Earles, D. S., Decker, G. L. and Lennarz, W. J. (1985). A monoclonal antibody inhibits calcium accumulation and skeleton formation in cultured embryonic cells of the sea urchin. *Cell* **41**, 639-648.
Cavalieri, V., Spinelli, G. and Di Bernardo, M. (2003). Impairing Otp homeodomain function in oral ectoderm cells affects skeletogenesis in sea urchin embryos. *Dev. Biol.* **262**, 107-118.
Cavalieri, V., Bernardo, M. D. and Spinelli, G. (2007). Regulatory sequences driving expression of the sea urchin Otp homeobox gene in oral ectoderm cells. *Gene Expr. Patterns* **7**, 124-130.
Cavalieri, V., Di Bernardo, M., Anello, L. and Spinelli, G. (2008). cis-Regulatory sequences driving the expression of the Hbox12 homeobox-containing gene in the presumptive aboral ectoderm territory of the *Paracentrotus lividus* sea urchin embryo. *Dev. Biol.* **321**, 455-469.
Cavalieri, V., Melfi, R. and Spinelli, G. (2009a). Promoter activity of the sea urchin (*Paracentrotus lividus*) nucleosomal H3 and H2A and linker H1 α-histone genes is modulated by enhancer and chromatin insulator. *Nucleic Acids Res.* **37**, 7407-7415.
Cavalieri, V., Di Bernardo, M. and Spinelli, G. (2009b). Functional studies of regulatory genes in the sea urchin embryo. *Methods Mol. Biol.* **518**, 175-188.
Chen, J. H., Luo, Y. J. and Su, Y. H. (2011). The dynamic gene expression patterns of transcription factors constituting the sea urchin aboral ectoderm gene regulatory network. *Dev. Dyn.* **240**, 250-260.
Chenna, R., Sugawara, H., Koike, T., Lopez, R., Gibson, T. J., Higgins, D. G. and Thompson, J. D. (2003). Multiple sequence alignment with the Clustal series of programs. *Nucleic Acids Res.* **31**, 3497-3500.
Croce, J., Lhomond, G., Lozano, J. C. and Gache, C. (2001). ske-T, a T-box gene expressed in the skeletogenic mesenchyme lineage of the sea urchin embryo. *Mech. Dev.* **107**, 159-162.
Cuykendall, T. N. and Houston, D. W. (2009). Vegetally localized Xenopus trim36 regulates cortical rotation and dorsal axis formation. *Development* **136**, 3057-3065.

Di Bernardo, M., Castagnetti, S., Bellomonte, D., Oliveri, P., Melfi, R., Palla, F. and Spinelli, G. (1999). Spatially restricted expression of PlOtp, a *Paracentrotus lividus* orthopedia-related homeobox gene, is correlated with oral ectodermal patterning and skeletal morphogenesis in late-cleavage sea urchin embryos. *Development* **126**, 2171-2179.
Diaz-Griffero, F., Vandegraaff, N., Li, Y., McGee-Estrada, K., Stremlau, M., Welikala, S., Si, Z., Engelman, A. and Sodroski, J. (2006). Requirements for capsids-binding and an effector function in TRIMCyp-mediated restriction of HIV-1. *Virology* **351**, 404-419.
Duboc, V., Röttinger, E., Besnardeau, L. and Lepage, T. (2004). Nodal and BMP2/4 signaling organizes the oral-aboral axis of the sea urchin embryo. *Dev. Cell* **6**, 397-410.
Duloquin, L., Lhomond, G. and Gache, C. (2007). Localized VEGF signaling from ectoderm to mesenchyme cells controls morphogenesis of the sea urchin embryo skeleton. *Development* **134**, 2293-2302.
Dupont, S., Zacchigna, L., Cordenonsi, M., Soligo, S., Adorno, M., Rugge, M. and Piccolo, S. (2005). Germ-layer specification and control of cell growth by Ectodermin, a Smad4 ubiquitin ligase. *Cell* **121**, 87-99.
Ettensohn, C. A. (1990). The regulation of primary mesenchyme cell patterning. *Dev. Biol.* **140**, 261-271.
Ettensohn, C. A. and Malinda, K. M. (1993). Size regulation and morphogenesis: a cellular analysis of skeletogenesis in the sea urchin embryo. *Development* **119**, 155-167.
Ettensohn, C. A. and Sweet, H. C. (2000). Patterning the early sea urchin embryo. *Curr. Top. Dev. Biol.* **50**, 1-44.
Ettensohn, C. A., Guss, K. A., Hodor, P. G. and Malinda, K. M. (1997). The morphogenesis of the skeletal system of the sea urchin embryo. In *Reproductive Biology of Invertebrates, Vol. 7: Progress in Developmental Biology* (ed. J. R. Collier), pp. 225-265. New Delhi. Calcutta: Oxford & IBH Publishing Co.
Ettensohn, C. A., Illies, M. R., Oliveri, P. and De Jong, D. L. (2003). Alx1, a member of the Cart1/Alx3/Alx4 subfamily of Paired-class homeodomain proteins, is an essential component of the gene network controlling skeletogenic fate specification in the sea urchin embryo. *Development* **130**, 2917-2928.
Finn, R. D., Mistry, J., Tate, J., Coggill, P., Heger, A., Pollington, J. E., Gavin, O. L., Gunasekaran, P., Ceric, G., Forslund, K. et al. (2010). The Pfam protein families database. *Nucleic Acids Res.* **38**, D211-D222.
Freemont, P. S. (1993). The RING finger. A novel protein sequence motif related to the zinc finger. *Ann. N. Y. Acad. Sci.* **684**, 174-192.
Gack, M. U., Shin, Y. C., Joo, C., Urano, T., Liang, C., Sun, L., Takeuchi, O., Akira, S., Chen, Z., Inoue, S. et al. (2007). TRIM25 RING-finger E3 ubiquitin ligase is essential for RIG-I-mediated antiviral activity. *Nature* **446**, 916-920.
Guss, K. A. and Ettensohn, C. A. (1997). Skeletal morphogenesis in the sea urchin embryo: regulation of primary mesenchyme gene expression and skeletal rod growth by ectoderm-derived cues. *Development* **124**, 1899-1908.
Gustafson, T. and Wolpert, L. (1967). Cellular movement and contact in sea urchin morphogenesis. *Biol. Rev. Camb. Philos. Soc.* **42**, 442-498.
Hardin, J. and Armstrong, N. (1997). Short-range cell-cell signals control ectodermal patterning in the oral region of the sea urchin embryo. *Dev. Biol.* **182**, 134-149.
Hardin, J., Coffman, J. A., Black, S. D. and McClay, D. R. (1992). Commitment along the dorsoventral axis of the sea urchin embryo is altered in response to NiCl2. *Development* **116**, 671-685.
Joazeiro, C. A. and Weissman, A. M. (2000). RING finger proteins: mediators of ubiquitin ligase activity. *Cell* **102**, 549-552.
Kudryashova, E., Kudryashov, D., Kramerova, I. and Spencer, M. J. (2005). Trim32 is a ubiquitin ligase mutated in limb girdle muscular dystrophy type 2H that binds to skeletal muscle myosin and ubiquitinates actin. *J. Mol. Biol.* **354**, 413-424.
Kurokawa, D., Kitajima, T., Mitsunaga-Nakatsubo, K., Amemiya, S., Shimada, H. and Akasaka, K. (1999). HpEts, an ets-related transcription factor implicated in primary mesenchyme cell differentiation in the sea urchin embryo. *Mech. Dev.* **80**, 41-52.
Lepage, T., Sardet, C. and Gache, C. (1992). Spatial expression of the hatching enzyme gene in the sea urchin embryo. *Dev. Biol.* **150**, 23-32.
Letunic, I., Doerks, T. and Bork, P. (2009). SMART 6, recent updates and new developments. *Nucleic Acids Res.* **37**, D229-D232.
Littlewood, D. T. and Smith, A. B. (1995). A combined morphological and molecular phylogeny for sea urchins (Echinoidea: Echinodermata). *Philos. Trans. R. Soc. Lond. B* **347**, 213-234.
Lupas, A. (1996). Coiled coils: new structures and new functions. *Trends Biochem. Sci.* **21**, 375-382.
Malinda, K. M., Fisher, G. W. and Ettensohn, C. A. (1995). Four-dimensional microscopic analysis of the filopodial behavior of primary mesenchyme cells during gastrulation in the sea urchin embryo. *Dev. Biol.* **172**, 552-566.
Meroni, G. and Diez-Roux, G. (2005). TRIM/RBCC, a novel class of 'single protein RING finger' E3 ubiquitin ligases. *BioEssays* **27**, 1147-1157.
Miller, J., Fraser, S. E. and McClay, D. (1995). Dynamics of thin filopodia during sea urchin gastrulation. *Development* **121**, 2501-2511.
Okazaki, K. (1975a). Normal development to metamorphosis. In *The Sea Urchin Embryo. Biochemistry and Morphogenesi* (ed. G. Cziahk), pp. 177-232. New York: Springer-Verlag.
Okazaki, K. (1975b). Spicule formation by isolated micromeres of the sea urchin embryo. *Am. Zool.* **15**, 567-581.
Oliveri, P., Carrick, D. M. and Davidson, E. H. (2002). A regulatory gene network that directs micromere specification in the sea urchin embryo. *Dev. Biol.* **246**, 209-228.
Oliveri, P., Tu, Q. and Davidson, E. H. (2008). Global regulatory logic for specification of an embryonic cell lineage. *Proc. Natl. Acad. Sci. USA* **105**, 5955-5962.
Perez-Caballero, D., Hatziioannou, T., Yang, A., Cowan, S. and Bieniasz, P. D. (2005). Human tripartite motif 5a domains responsible for retrovirus restriction activity and specificity. *J. Virol.* **79**, 8969-8978.
Ransick, A., Rast, J. P., Minokawa, T., Calestani, C. and Davidson, E. H. (2002). New early zygotic regulators expressed in endomesoderm of sea urchin embryos discovered by differential array hybridization. *Dev. Biol.* **246**, 132-147.
Revilla-i-Domingo, R., Oliveri, P. and Davidson, E. H. (2007). A missing link in the sea urchin embryo gene regulatory network: hesC and the double-negative specification of micromeres. *Proc. Natl. Acad. Sci. USA* **104**, 12383-12388.
Röttinger, E., Besnardeau, L. and Lepage, T. (2004). A Raf/MEK/ERK signaling pathway is required for development of the sea urchin embryo micromere lineage through phosphorylation of the transcription factor Ets. *Development* **131**, 1075-1087.
Röttinger, E., Croce, J., Lhomond, G., Besnardeau, L., Gache, C. and Lepage, T. (2006). Nemo-like kinase (NLK) acts downstream of Notch/Delta signalling to downregulate TCF during mesoderm induction in the sea urchin embryo. *Development* **133**, 4341-4353.
Röttinger, E., Saudemont, A., Duboc, V., Besnardeau, L., McClay, D. and Lepage, T. (2008). FGF signals guide migration of mesenchymal cells, control skeletal morphogenesis [corrected] and regulate gastrulation during sea urchin development. *Development* **135**, 353-365.
Saudemont, A., Haillot, E., Mekpoh, F., Bessodes, N., Quirin, M., Lapraz, F., Duboc, V., Röttinger, E., Range, R., Oisel, A. et al. (2010). Ancestral regulatory circuits governing ectoderm patterning downstream of nodal and BMP2/4 revealed by gene regulatory network analysis in an echinoderm. *PLoS Genet.* **6**, e1001259.
Sharma, T. and Ettensohn, C. A. (2010). Activation of the skeletogenic gene regulatory network in the early sea urchin embryo. *Development* **137**, 1149-1157.
Short, K. M. and Cox, T. C. (2006). Subclassification of the RBCC/TRIM superfamily reveals a novel motif necessary for microtubule binding. *J. Biol. Chem.* **281**, 8970-8980.
Solursh, M. and Lane, M. C. (1988). Extracellular matrix triggers a directed cell migratory response in sea urchin primary mesenchyme cells. *Dev. Biol.* **130**, 397-401.
Su, Y. H. (2009). Gene regulatory networks for ectoderm specification in sea urchin embryos. *Biochim. Biophys. Acta* **1789**, 261-267.
Summerton, J. and Weller, D. (1997). Morpholino antisense oligomers: design, preparation, and properties. *Antisense Nucleic Acid Drug Dev.* **7**, 187-195.
Sweet, H. C., Gehring, M. and Ettensohn, C. A. (2002). LvDelta is a mesoderm-inducing signal in the sea urchin embryo and can endow blastomeres with organizer-like properties. *Development* **129**, 1945-1955.
Thisse, B., Heyer, V., Lux, A., Alunni, V., Degrave, A., Seiliez, I., Kirchner, J., Parkhill, J. P. and Thisse, C. (2004). Spatial and temporal expression of the zebrafish genome by large-scale in situ hybridization screening. *Methods Cell Biol.* **77**, 505-519.
Tuoc, T. C. and Stoykova, A. (2008). Trim11 modulates the function of neurogenic transcription factor Pax6 through ubiquitin-proteosome system. *Genes Dev.* **22**, 1972-1986.
Wilt, F. H. (2002). Biomineralization of the spicules of sea urchin embryos. *Zool. Sci.* **19**, 253-261.
Yoshigai, E., Kawamura, S., Kuhara, S. and Tashiro, K. (2009). Trim36/Haprin plays a critical role in the arrangement of somites during *Xenopus* embryogenesis. *Biochem. Biophys. Res. Commun.* **378**, 428-432.